C–S Bond Formation

Carbon–Sulfur Bond Formation between a Ruthenium-Coordinated Thiyl Radical and Methyl Ketones**

Selma Poturovic, Mark S. Mashuta, and
Craig A. Grapperhaus*

The oxidation of metal–thiolate complexes to yield disulfides is well-known.[1–4] This process may be irreversible, as with the oxidation of $[Fe(SPh)(CO)(PPh_3)(\eta^5\text{-}C_5H_5)]PF_6$ to form the disulfide-bridged binuclear product $[(Fe(CO)(PPh_3)(\eta^5\text{-}C_5H_5)_2(\mu\text{-}SSPh_2)]^{2+}$,[5] or reversible, as with the oxidation of ($[Ru^{III}L]$, L = 1,4,7-tris(4-*tert*-butyl-2-mercaptobenzyl)-1,4,7-triazacyclononane), which yields an isolable, intermolecular disulfide complex.[6] In both cases, the oxidation is consistent with a metal–thiyl radical intermediate. Recent efforts have focused on stabilizing metal-coordinated thiyl radicals.[7–10] Wieghardt and co-workers synthesized and compared phenylthiyl and phenoxyl radicals coordinated to Co^{III} centers (and other metal centers) with tacn-based ligands (tacn = 1,4,7-triazacyclononane).[7] The phenylthiyl radical displays increased reactivity compared with the phenoxyl analogue. In the former the unpaired electron is localized on the sulfur

---

[*] S. Poturovic, Dr. M. S. Mashuta, Prof. Dr. C. A. Grapperhaus
Department of Chemistry
University of Louisville
Louisville, KY 40292 (USA)
Fax: (+1) 502-852-8149
E-mail: grapperhaus@louisville.edu

[**] This research was supported by the National Science Foundation (CHE-0238137). CCD X-ray equipment was purchased through funds provided by the Kentucky Research Challenge Trust Fund.

Supporting information for this article is available on the WWW under http://www.angewandte.org or from the author.

DOI: 10.1002/ange.200462713

atom, whereas in the latter the electron delocalizes over the phenyl ring. Earlier Hückel molecular orbital (MO) calculations by Darensbourg and co-workers for RS·[{Cr(CO)$_5$}$_2$], in which R is a *tert*-butyl group, also conclude that the singly occupied molecular orbital (SOMO) is concentrated largely on the 3p orbital of the sulfur atom.[11] Moreover, the unpaired electron in noncoordinated thiyls is also localized on the sulfur atom as confirmed by recent density functional theory (DFT) calculations of the cysteine-derived radical.[12] As expected, localization leads to enhanced reactivity. For example, phenylthiyl radicals decay at a rate of approximately $10^9\,\text{M}^{-1}\,\text{s}^{-1}$ to disulfide.[13]

Herein, we report the novel reactivity of an electrophilic, oxidized metal–thiolate (metal-coordinated thiyl radical) with ketones that results in C–S bond formation. Electrophilic behavior contrasts the well-studied reactivity of nucleophilic metal–thiolates and presents a new method for the synthesis of metal–sulfur complexes.[14] Previously, we reported the oxidation of [Ru(dppbt)$_3$] (**2**; dppbt = 2-diphenylphosphinobenzenethiolate) in acetonitrile to form the observable metal-coordinated Ru^{III}–thiyl radical complex **3**.[15] In this case, complex **3** is short-lived and decays to form the proposed Ru^{II}–disulfide complex **4**. The overall oxidation of **2** to **4** proceeds by a coupled two-electron ligand oxidation and one-electron metal-centered reduction. At an applied potential of 620 mV, an EC mechanism (EC is short for electrode step–chemical step) is observed. Complex **4** can be further oxidized to its Ru^{III} derivative, **5**, but only at more positive potentials (+806 mV).

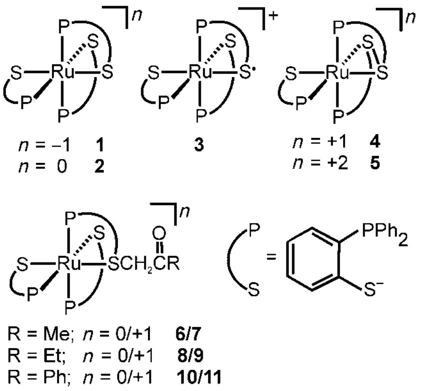

Oxidation of **2** at 620 mV in acetone or related ketones also initially yields **3**. At this point, the pathways in acetonitrile and ketones diverge as shown in Scheme 1. Decay of **3** in ketones results in C–S bond formation between the thiyl radical and the solvent molecule to yield the Ru^{II}–thioether product **6** (in acetone). Further oxidization to Ru^{III} (formation of **7**) occurs at the potential applied to the cell. Thus, the oxidation of **2** to **7** is a two-electron ECE (electrode–chemical–electrode) process with no change in the formal oxidation state of the metal center and C–S bond formation.

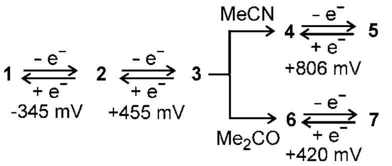

Scheme 1. Oxidation pathways for **1** in acetonitrile (top) and acetone (bottom).

The oxidation of **2** in acetone was performed by bulk electrolysis in a controlled-temperature electrochemical cell ($T = -17\,°C$) equipped with a quartz window for in situ UV/Vis monitoring. On the basis of coulometric measurements and UV/Vis spectroscopy (Figure 1), the oxidation is unequivocally assigned as two electrons per metal center, which is in contrast to the one-electron oxidation of **2** in acetonitrile to give **4**. During initial stages of the oxidation in acetone, the charge-transfer bands of **2** at 540 and 1041 nm decrease in intensity with a concomitant increase in intensity at 850 nm, which is attributed to the formation of **3**. This observation for the oxidation in acetone is identical to that for the oxidation in acetonitrile.[15] However, upon decay of the band at 850 nm, a new band at 735 nm, which is assigned to complex **7**, emerges in stark contrast to the silent visible spectrum in acetonitrile associated with **4**.

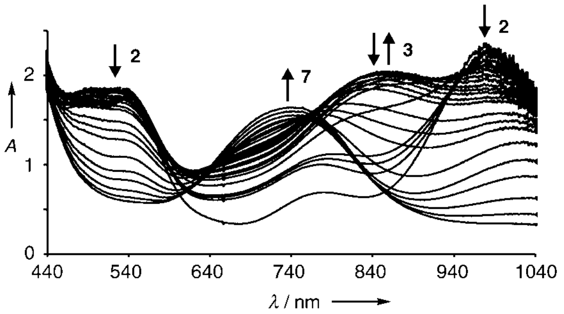

Figure 1. Electronic spectra obtained during bulk oxidation of **2** to **7** at 620 mV in acetone at −17 °C. Data were collected every 50 mC (0.10 electron equivalents).

Square-wave voltammograms recorded after bulk oxidation of **2** in acetonitrile and acetone are consistent with the assignments of **4** as Ru^{II}–disulfide and **7** as Ru^{III}–thioether (Figure 2). UV/Vis-monitored spectroelectrochemistry confirms a reversible one-electron reduction of **7** to give **6** at an applied potential of +200 mV (see Supporting Information). The Ru^{III}/Ru^{II} couple of **7**/**6** is shifted by +813 mV relative to the thiolato precursors **2**/**1**, consistent with previously reported shifts associated with S alkylation.[16] In contrast, a shift of +1151 mV in the Ru^{III}/Ru^{II} potential for the disulfide complexes **5**/**4** indicates the modification of two anionic thiolates to form two neutral sulfur donors. All complexes assigned as Ru^{III} display rhombic electron paramagnetic resonance (EPR) spectra with g values near 2 as shown in Table 1. The notable exception is the metal-coordinated radical **3**, which is EPR-silent, consistent with the coupling of the ruthenium spin ($S = 1/2$) with that of the thiyl radical ($S = 1/2$).

The electrospray-ionization mass spectrum (ESI-MS) of complex **7** displays a parent ion with $m/z = 1038$, which is consistent with the proposed structure (see Supporting

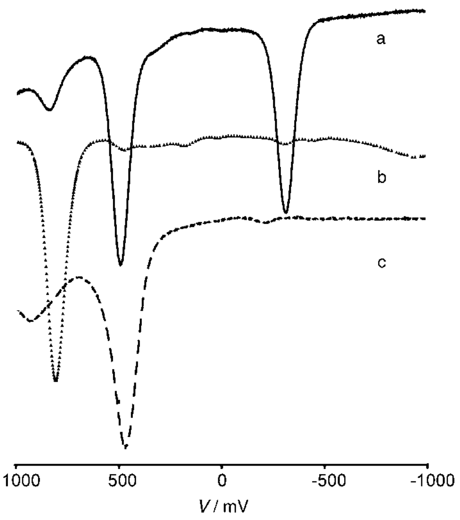

Figure 2. Comparison of square-wave voltammograms for solutions of a) **1**/**2** (1 mM) in acetonitrile, b) **4**/**5** (1 mM) in acetonitrile, and c) **6**/**7** (1 mM) in acetone. Voltammograms were obtained at a glassy carbon electrode referenced versus Ag^+/Ag^0.

Table 1: Formal oxidation-state assignments, charge-transfer (CT) band energies, and EPR *g* values for **1**–**11**.

Complex	Formal oxidation state	CT absorbance λ_{max} (ε)	*g* values[a]
1	II	–	–
2	III	1041 (3020)[b]	2.12, 2.06, 2.04
3	III	850 (4800)	–
4	II	–	–
5	III	688 (2338)	2.09, 2.05, 2.03
6	II	–	–
7	III	735 (1921)[c]	2.09, 2.04, 2.01
8	II	–	–
9	III	707 (557)[d]	2.15, 2.04, 2.02
10	II	–	–
11	III	697 (106)[e]	2.15, 2.06, 2.01

[a] Obtained from frozen solution at 77 K. [b] Acetonitrile solution at −17 °C. [c] Acetone solution at −17 °C. [d] 2-Butanone solution at −17 °C. [e] Acetophenone solution recorded at 19 °C.

Information). Complex **6**, the Ru^{II} derivative of **7**, was also prepared chemically by alkylation of **1** with chloroacetone in acetonitrile. The ESI-MS, UV/Vis, spectroelectrochemical, and EPR measurements of **7**/**6** from the two routes are indistinguishable, which is consistent with the oxidation-induced C–S bond formation and the proposed structures given above.

The X-ray crystal structure of **6**[17–22] (Figure 3)[23] confirms the alkylation of a single sulfur site to yield a neutral ruthenium complex in a triphosphine-dithiolate-thioether donor set. The chelating ligands arrange in a meridional fashion as seen in **1** and its methylene-bridged dialkylated derivative $[Ru(dppbt)\{CH_2(dppbt)_2\}]^+$ (**14**).[24] The ketone functional group of the thioether donor is directed away from the metal center. The Ru–P bond lengths range from 2.2939(11) to 2.3626(10) Å, similar to the bonds in **1** and **14**. The $Ru{-}S_{thiolate}$ bond lengths for Ru–S1, 2.3971(10) Å, and Ru–S2, 2.3826(10) Å, in **6** are not significantly shorter than the $Ru{-}S_{thioether}$ bond length for Ru–S3, 2.4151(10) Å, as is the case in **14**.

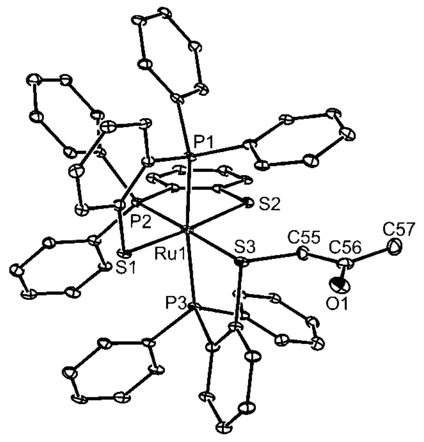

Figure 3. ORTEP representation of **6** (thermal ellipsoids are set at the 40% level of probability).[23] Chlorobenzene molecules have been omitted. Selected bond lengths [Å] and angles [°]: Ru-P1 2.3545(10), Ru-P2 2.2939(11), Ru-P3 2.3626(10), Ru-S1 2.3971(10), Ru-S2 2.3826(10), Ru-S3 2.4151(10), S3-C55 1.813(4); P2-Ru-P1 95.00(4), S2-Ru-P1 90.16(4), S2-Ru-S1 175.57(4), C55-S3-Ru 108.98(13).

Scheme 2 details a proposed pathway for the reaction of **3** with acetone.[25] The enol tautomer of acetone acts as a nucleophile and attacks the metal-coordinated thiyl radical to result in the reduction of the Ru^{III} center to Ru^{II}. Deprotonation of the Ru^{II} species yields the Ru^{II}–thioether product **6**. At the potentials necessary for oxidation of **2** to form **3**, **6** is further oxidized to the observed product **7**. To support this pathway, **2** was oxidized in the presence of the trimethylsilyl enol ether derivative of acetone. The oxidation is a two-electron process and yields a product identified spectroscopically as **7**. Notably, no thiyl radical intermediate is observed that is consistent with the expected rate increase with increased enol concentration.

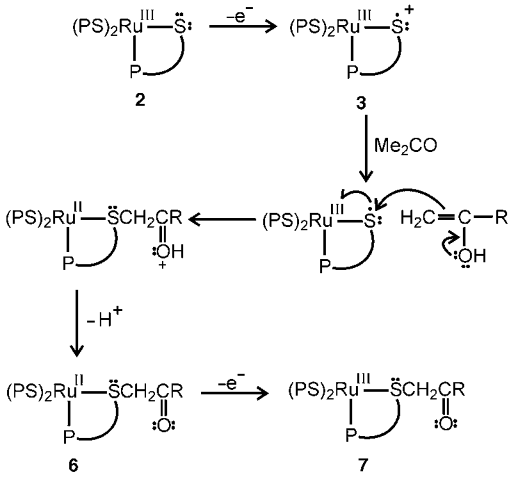

Scheme 2. Proposed pathway for the oxidation of **2** in acetone.

To support the pathway proposed in Scheme 2, **3** was generated under a variety of conditions. Similar ketones (2-

butanone and acetophenone) generate products that are closely related to **6** and **7** (see complexes **8**–**11**; Ph = phenyl). Acetonitrile, malononitrile, or THF, which have C–H bond enthalpies similar to or lower than that of acetone, but are not enolizable, yield only Ru^{II}–disulfide **4** and there is no C–S bond formation.[26] Thus, a pathway that involves an initial hydrogen atom abstraction step is not consistent with the observed data.

The reaction of **3** with ketones resembles the previously noted reactivity of disulfide-bridged metal clusters with acetone.[27,28] C–S bond formation was observed at the bridging disulfide upon addition of acetone. It was suggested that the enol tautomer of acetone acts as a nucleophile and attacks the disulfide, whereas the cluster is reduced by two electrons. This reduction is spread over two metal centers.

Finally, the C–S bond formation between the enol tautomer of acetone and **3** is reminiscent of the reaction between ethylene and nickel dithiolene reported by Stiefel and co-workers (Scheme 3).[29] In both cases, an oxidized mononuclear metal–sulfur complex is attacked by an ene nucleophile, which results in reduction at the metal center and C–S bond formation. Reduction of the nickel center promotes C–S bond cleavage and release of ethylene. Further studies by Geiger on related systems revealed that reductive dissociation of the olefin proceeds by a two-electron ECE mechanism.[30] Current efforts are focusing on the reaction of **3** with additional substrates.

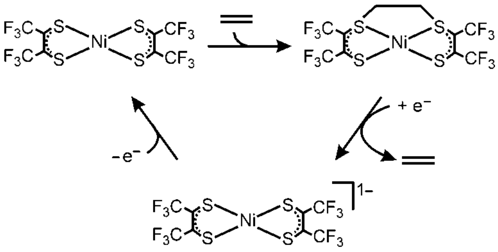

Scheme 3. Reversible ethylene binding to nickel dithiolene.[29]

Experimental Section

Physical and Spectroscopic Methods**:** IR spectra were obtained by using a Thermo Nicolet Avatar 360 spectrometer with a 4 cm^{-1} resolution. X-band EPR spectra were collected on a Bruker EMX EPR spectrometer at 77 K in a Suprasil quartz dewar. Spectra were simulated with SimFonia. An Agilent 8453 diode array spectrometer was used for electronic absorption spectroscopy. Elemental analyses were performed by Midwest Microlab (Indianapolis). Mass spectra were recorded at the University of Louisville Mass Spectrometry Core Laboratory. All electrochemical experiments were performed with an EG&E 273 potentiostat/galvenostat. Electrochemical and spectroelectrochemical measurements were carried out in the 10 mL cell designed by E. Böthe of the Max Planck Institute für Bioanorganische Chemie, Mülheim (Germany), as described previously.[15]

Synthetic Methods: Syntheses of complexes **1**–**5** have been previously reported.[15,24] 2-Butanone, and acetophenone were purchased from Aldrich and were freshly distilled immediately prior to use. Syntheses were performed under a N_2 atmosphere by using standard Schlenk techniques unless otherwise stated. Chloroacetone, chlorotrimethylsilane, sodium iodide, and triethylamine were obtained from Aldrich and used as received. (Isopropenyloxy)trimethylsilane was prepared according to published methods.[31]

6: Chloroacetone (0.015 g, 16 mmol) was added with a microsyringe to a yellow solution of **1** (0.188 g, 12.4 mmol) in acetonitrile (100 mL). The reaction solution was stirred for 1 hour. Removal of solvent under reduced pressure yielded a yellow residue. The crude product was dissolved in THF and gravity filtered to remove residual PPNCl. Removal of solvent from the filtrate yielded **6** in 43 % yield. X-ray-quality needle-like crystals were obtained from liquid diffusion of chlorobenzene/ether. Elemental analysis (%) calcd for $C_{57}H_{47}OP_3S_3Ru$: C 65.94, H 4.56, found: C 63.48, H 4.37; IR (KBr pellet): $\tilde{\nu}$3047(m), 1707(m), 1429(m), 1082(s), 693(s), 518 cm^{-1} (s). Compound **6** can also be prepared by electrochemical reduction of **7** in acetone (1 mM, -17 ± 3 °C) at an applied potential of +200 mV.

7: Bulk oxidation of **3** in acetone at 620 mV (−17 °C) yields **7** by a two-electron oxidation. The product was characterized by UV/Vis and EPR spectroscopy, and square-wave voltammetry. Electronic absorption: $\lambda_{max} = 735$ nm ($\varepsilon = 1921$ cm^{-1}M^{-1}).

Received: November 24, 2004

Keywords: ketones · radicals · ruthenium · sulfur

[1] M. T. Ashby, J. H. Enemark, D. L. Lichtenberger, *Inorg. Chem.* **1988**, *27*, 191.
[2] C. A. Grapperhaus, M. Y. Darensbourg, *Acc. Chem. Res.* **1998**, *31*, 451.
[3] L. E. Maelia, M. Millar, S. A. Koch, *Inorg. Chem.* **1992**, *31*, 4594.
[4] J. C. Noveron, R. Herradora, M. M. Olmstead, P. K. Mascharak, *Inorg. Chim. Acta* **1999**, *285*, 269.
[5] P. M. Treichel, L. D. Rosenhein, *Inorg. Chem.* **1984**, *23*, 4018.
[6] B. Albela, E. Bothe, O. Brosch, K. Mochizuki, T. Weyhermüller, K. Wieghardt, *Inorg. Chem.* **1999**, *38*, 5131.
[7] S. Kimura, E. Bill, E. Bothe, T. Weyhermüller, K. Wieghardt, *J. Am. Chem. Soc.* **2001**, *123*, 6025.
[8] D. Herebian, E. Bothe, E. Bill, T. Weyhermüller, K. Wieghardt, *J. Am. Chem. Soc.* **2001**, *123*, 10012.
[9] P. Ghosh, E. Bill, T. Weyhermüller, F. Neese, K. Wieghardt, *J. Am. Chem. Soc.* **2003**, *125*, 1293.
[10] C. H. Hsieh, I. J. Hsu, C. M. Lee, S. C. Ke, T. Y. Wang, G. H. Lee, Y. Wang, J. M. Chen, J. F. Lee, W. F. Liaw, *Inorg. Chem.* **2003**, *42*, 3925.
[11] J. Springs, C. P. Janzen, M. Y. Darensbourg, J. C. Calabrese, P. J. Krusic, J. N. Verpeaux, C. Amatore, *J. Am. Chem. Soc.* **1990**, *112*, 5789.
[12] M. van Gastel, W. Lubitz, G. Lassmann, F. Neese, *J. Am. Chem. Soc.* **2004**, *126*, 2237.
[13] G. N. R. Tripathi, Q. Sun, D. A. Armstrong, D. M. Chipman, R. H. Schuler, *J. Phys. Chem.* **1992**, *96*, 5344.
[14] E. C. Constable, *Metals and Ligand Reactivity*, *2nd ed.*, VCH, Weinheim, **1996**.
[15] C. A. Grapperhaus, S. Poturovic, *Inorg. Chem.* **2004**, *43*, 3292.
[16] P. J. Farmer, J. H. Reibenspies, P. A. Lindahl, M. Y. Darensbourg, *J. Am. Chem. Soc.* **1993**, *115*, 4665.
[17] Crystal data for **6**: yellow needle, orthorhombic, space group *Pbca*, $a = 24.832(2)$, $b = 10.9955(10)$, $c = 41.949(4)$ Å, $V = 11453.7(18)$ Å^3, $\rho_{calcd} = 1.465$ g cm^{-3}, $Z = 8$. Data were collected on a Bruker SMART APEX CCD using $Mo_{K\alpha}$ radiation. For all 13702 unique reflections (R(int) = 0.056), the final anisotropic full-matrix least-squares refinement on F^2 for 713 variables data converged at $R1 = 0.06$ and $wR2 = 0.11$ with a GOF of 1.09. CCDC-256671 contains the supplementary crystallographic data for this paper. These data can be obtained free of charge from

The Cambridge Crystallographic Data Centre via www.ccdc.cam.ac.uk/data_request/cif.

[18] SHELXL-97. Program for the Refinement of Crystal Structures, University of Göttingen, Germany, **1997**.

[19] SHELXTL (v6.12), Program Library for Structure Solution and Molecular Graphics, Bruker Advanced X-ray Solutions, Inc., Madison, WI, **2001**.

[20] SMART (v.5628), Bruker Advanced X-ray Solutions, Inc., Madison, WI, **2002**.

[21] SAINT (v6.36), Bruker Advanced X-ray Solutions, Inc., Madison, WI, **2002**.

[22] SADABS (v2.02), Area Detector Absorption Correction, University of Göttingen, Germany, **2001**.

[23] ORTEP-3 for Windows: L. J. Farrugia, *J. Appl. Crystallogr.* **1997**, *30*, 565.

[24] C. A. Grapperhaus, S. Poturovic, M. S. Mashuta, *Inorg. Chem.* **2002**, *41*, 4309.

[25] An alternate pathway in which complex **3** is regarded as a $\mathrm{Ru}^{\mathrm{IV}}$–thiolate would yield the same product. Attack by the enol tautomer at sulfur would result in the two-electron reduction of the metal. The radical pathway is favored based on the spectroscopic assignment of **3** as a metal-coordinated thiyl radical[15] and the high sulfur character in the HOMO of nucleophilic metal thiolates.[1]

[26] J. A. Kerr, *Chem. Rev.* **1966**, *66*, 465.

[27] A. Venturelli, T. B. Rauchfuss, A. K. Verma, *Inorg. Chem.* **1997**, *36*, 1360.

[28] K. Matsumoto, H. Sugiyama, *Acc. Chem. Res.* **2002**, *35*, 915.

[29] K. Wang, S. E. Stiefel, *Science* **2001**, *291*, 106.

[30] W. E. Geiger, *Inorg. Chem.* **2002**, *41*, 1360.

[31] P. Cazeau, F. Duboudin, F. Moulines, O. Babot, J. Dunogues, *Tetrahedron* **1987**, *43*, 2075.